Measurements of the Flow Around a Lifting-Wing/Body Junction

D. H. Wood* and R. V. Westphal†
NASA Ames Research Center, Moffett Field, California 94035

Detailed measurements of all three mean velocity components and five of the six Reynolds stresses have been made around a model of a lifting-wing/body junction. The body was the flat working section floor of a small blower wind tunnel. Measurements of the surface pressure distribution on the NACA 0012 wing showed that the lift coefficient at the body surface was reduced by only 16% from the freestream value. It is shown that the near constancy of the bound vorticity requires the formation of axial vorticity within the body boundary layer. This vorticity was concentrated in the two legs of the necklace vortex formed near the leading edge of the wing. The magnitude of the vorticity was always greater in the leg that developed on the suction surface. By four chord lengths downstream of the trailing edge, the turbulence structure of the suction leg was qualitatively similar to that of a single vortex imbedded in a turbulent boundary layer.

Nomenclature

C_f = skin friction coefficient, $\tau/(1/2\rho U_o^2)$
C_l = section lift coefficient, $L/(1/2c\rho U_o^2)$
C_P = pressure coefficient, $[P(x) - P_o]/(1/2\rho U_o^2)$
c = airfoil chord, 10 cm
H = streamwise distance from vortex center to measurement plane
L = lift per unit span
P = static pressure
Re_c = Reynolds number based on U_o and c, $U_o c/\nu$
Re_θ = boundary-layer momentum thickness Reynolds number, $U_e\theta/\nu$
U, V, W = mean velocity components in X, Y, Z directions, respectively
u, v, w = fluctuating velocity components in X, Y, Z directions, respectively
X, Y, Z = right-hand Cartesian streamwise, normal, and cross-stream coordinate directions, respectively; origin at airfoil midchord and made dimensionless using the airfoil chord
x = distance along the airfoil chord line from leading edge
Y_w, Z_w = Y and Z boundaries on measurement planes, respectively
α = airfoil angle of attack
γ_c = partial circulation
γ_m = measured partial circulation, $\gamma_m(X,Y) = \int_{-Z_w}^{Z_w} W(Y, Z)\, dZ$
δ_{99} = undisturbed boundary-layer momentum thickness, defined as the height where $U/U_e = 0.99$
θ = undisturbed boundary-layer momentum thickness
ν, ρ = fluid kinematic viscosity and density, respectively
τ = skin friction
Ω_X = streamwise vorticity
$(\ )_o$ = reference value (measured at $X = -14$)
$(\ )_e$ = quantity in the freestream

I. Introduction

ACCORDING to Bradshaw,[1,2] the most common cause of secondary motion in an initially two-dimensional turbulent shear layer is the inviscid skewing of mean vortex lines as the layer encounters an obstacle or is otherwise deflected. In other words, the skewing produces a secondary, streamwise vorticity component Ω_X from the upstream vorticity lying entirely in the cross-stream direction. The predominantly skew-induced secondary flow around and behind a nonlifting-wing/body junction has been studied extensively, e.g., Shabaka and Bradshaw,[3] Nakayama and Rahai,[4] Kubendran et al.,[5] and Mehta.[6] By comparison, the more complex and aerodynamically relevant flow around the junction between a *lifting* wing and a body has received little attention, e.g., Hawthorne,[7] Young,[8] Barber,[9] and Özcan and Ölcmen.[10] In this case, any vorticity shed from the wing near the body should provide an additional contribution to the secondary flow. The disturbed body boundary layer can be of considerable aerodynamic importance. For example, the fuselage boundary layer downstream of the wing can interact with the tail plane and then influence the vorticity trailing from the fuselage.[8] As far as we are aware, the disturbed boundary layer has not been studied, either in terms of the turbulence structure or the vorticity distribution and its interaction with the lift distri-

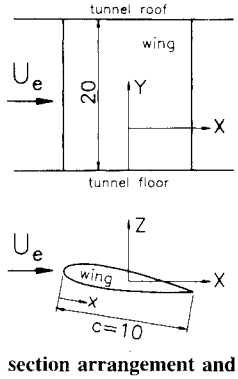

Fig. 1 Test section arrangement and coordinates.

Received Jan. 10, 1990; revision received Jan. 17, 1991; accepted for publication Jan. 17, 1991.

*Fluid Mechanics Research Branch; Senior Lecturer on leave from Department of Mechanical Engineering, University of Newcastle, NSW, 2308, Australia.

†Fluid Mechanics Research Branch; currently Associate Professor, Mechanical Engineering Department, San Jose State University, San Jose, CA 95192.

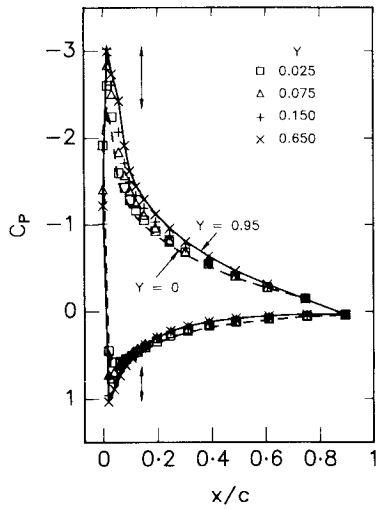

Fig. 2 Airfoil pressure distributions at varying heights above the floor: vertical arrows indicate change in maximum and minimum C_P between $Y = 0$ and 0.95.

bution. Kuchemann,[11] for example, pointed out the possibility of an inviscid alteration to the lift because the singularity distribution needed to model the body surface will be changed in the presence of a wing. This in turn can influence the wing's surface pressure distribution in a manner that is difficult to quantify. If a round body approximating a fuselage is added to an isolated wing, the lift of the wing is usually increased as the junction is approached and the fuselage itself contributes to the lift.[12]

In the present context, the skewing just referred to occurs in the immediate vicinity of the junction. It is worth noting that, in cascades and other geometries where the mean flow changes direction, the whole boundary layer can be skewed over its entire cross-stream extent. This contributes strongly to the so-called passage vortex, which dominates the secondary motion in cascades, e.g., Moore and Ransmyr,[13] but has no counterpart for isolated airfoils. The large literature on cascades is, therefore, not directly relevant to the present study.

Here we report on wing pressure distributions and mean flow measurements for an unswept NACA 0012 section mounted normally to the flat floor of a conventional wind tunnel (simulating the body) at an angle of attack $\alpha = 10$ deg. This angle was chosen to provide a high C_l without complications, such as large laminar separation bubbles that may occur at low chord Reynolds numbers Re_c. In addition, the secondary velocities and Reynolds stresses could be measured accurately with an X wire without aligning its axis to the local mean flow direction. Some turbulence measurements will be presented later, with the primary aim of comparing the turbulence structure to that of simpler cases of secondary motion in otherwise two-dimensional boundary layers, e.g. Shabaka et al.,[14] Mehta and Bradshaw,[15] Westphal et al.,[16,17] Westphal and Mehta,[18] and Pauley and Eaton.[19]

The small scale of the experiment and low velocity range of the wind tunnel caused two major limitations. First, we could not easily study the parametric variation of, say, Reynolds number or the ratio of undisturbed body boundary-layer thickness to airfoil chord. Second, we were unable to investigate the skewing of the upstream velocity close to the leading edge of the airfoil. However, the high degree of uniformity and two dimensionality of the undisturbed flow and the ease and accuracy with which we could establish the test conditions and probe the flow allowed the investigation of the relationship between the secondary motion and the lift on the wing that forms a major part of this paper. The measurement techniques used are described in the next section. That is followed by the results and discussion in Sec. III and a summary of conclusions in Sec. IV.

II. Experimental Apparatus

Figure 1 shows a schematic of the experiment and defines the coordinate directions. The wind tunnel was designed and employed by R. V. Westphal for several previous studies; it is described by Westphal[20] and Wood and Westphal.[21] The airfoil had a NACA 0012 section and a chord $c = 10$ cm. It spanned the 20 cm between the floor and roof of the 20 × 80 × 300-cm test section, and so caused negligible solid blockage. The midchord and midspan position coincided with the geometric center of the test section ($X = 0$, $Y = 1$, $Z = 0$; throughout this paper, uppercase symbols indicate lengths made dimensionless using the airfoil chord). We will refer to the Y direction as spanwise and to the Z direction as cross stream. Furthermore, the use of boundary layer without qualification will imply the floor boundary layer; note that the floor and ceiling boundary layers are nominally identical.

The freestream reference velocity U_o was 27.5 m/s, giving a chord Reynolds number Re_c of 1.8×10^5 for the test section conditions that were atmospheric static pressure and room temperature in this open return wind tunnel. The boundary layer on the wing was not tripped, but the floor and ceiling layers were each tripped using a wire of 0.4-mm diam positioned at $X = -13.0$ (20 cm downstream of the contraction exit). The height and width of the working section were constant with X, resulting in a small favorable pressure gradient in the empty tunnel. The undisturbed boundary-layer parameters at $X = 0.15$ for $U_o = 27.5$ m/s are $Re_\theta = 4200$, $C_f = 0.0030$, and $\delta_{99} = 2.2$ cm. The latter will be used as an estimate of the thickness of the disturbed boundary layer in a later discussion.

Two airfoils (with the same section and chord) were used at different stages of the experiments. They were inserted through a specially machined slot in a circular disk in the floor and then rotated about the midchord position ($X = 0$) to the required α. The first wing had no pressure tappings and could be retracted to allow X-wire calibration. It had a flat top that was carefully butted against the tunnel roof before obtaining the flow measurements. The second, a pressure tapped airfoil, could also slide through another slotted disk in the suitably modified ceiling. The single line of 30 pressure tappings, each of about 1-mm diam, could thus be set to any height while keeping α constant.

The uniformity of the undisturbed U_o at $X = 0$ was better than 0.25% and the maximum angularity was 0.25 deg. The properties of the freestream fluctuations at 20 m/s were doc-

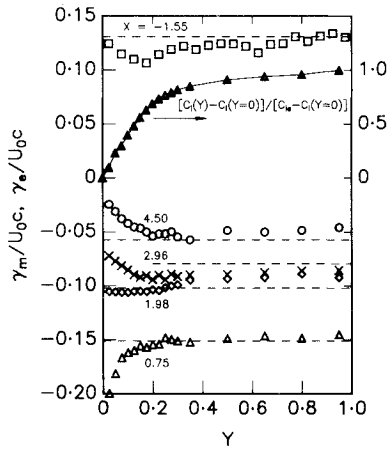

Fig. 3 Partial circulation integrals γ_m (Y) at different streamwise locations: open symbols show $\gamma_m(Y)$ for the values of X; dashed lines indicate γ_e; solid symbols show $[C_l(Y) - C_l(Y = 0)]/[C_{l_e} - C_l(Y = 0)]$.

umented by Wood and Westphal[21]: the total rms of the fluctuating streamwise velocity was about 0.21% of U_e and consisted of a one-dimensional unsteadiness component of about 0.18% and a nearly isotropic turbulence component of 0.11%. These values fell slightly with increasing U_e. Detailed surveys of the undisturbed boundary layer performed by Westphal for previous studies (e.g., Ref. 17) showed spanwise variations in C_f of about 8% over the center half-span, indicative of a reasonably two-dimensional boundary layer on the tunnel floor.

The symmetry of the experimental setup was checked in two ways. First, an X wire was traversed through the undisturbed ceiling and floor boundary layers at $X = 1.5$. The good agreement for all mean boundary-layer parameters and turbulence quantities justified the assumption of symmetry

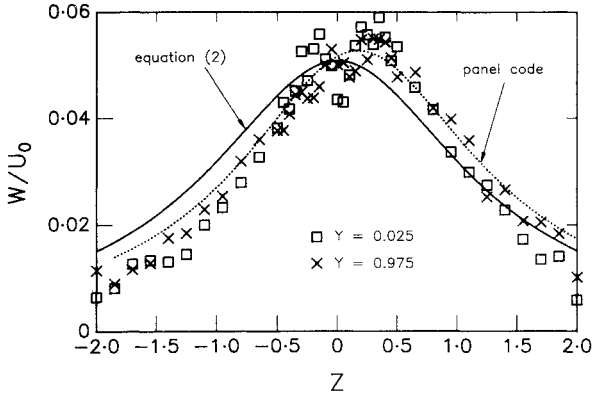

a) $X = -1.55$

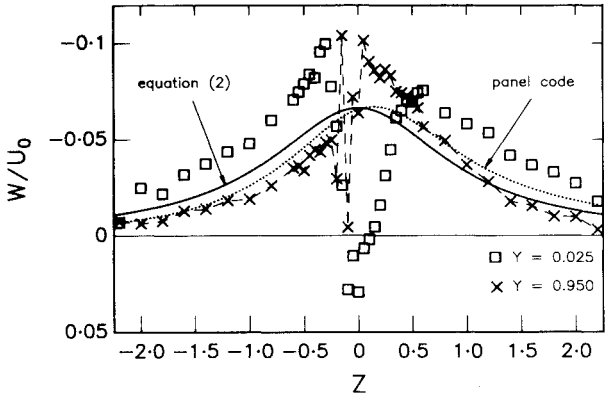

b) $X = 0.75$ (dashed line joins points for $Y = 0.95$ for visual aid only)

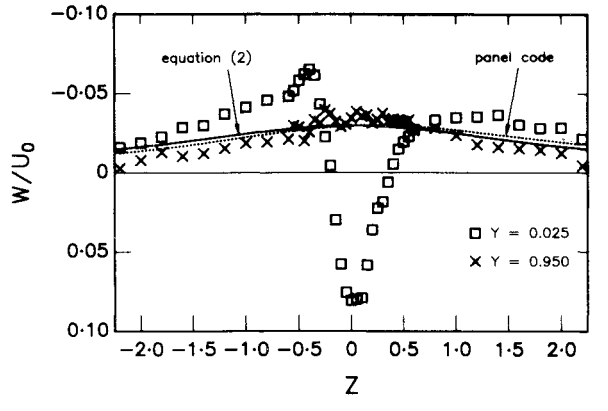

c) $X = 1.98$

Fig. 4 Spanwise profiles of W/U_o: symbols show measured W/U_o for values of Y; solid lines show W/U_o from Eq. (2); dotted lines show W/U_o from the panel code calculations.

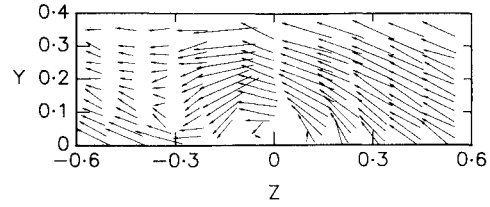

a) $X = 0.75$ (measurements for every second value of Z have been omitted for clarity)

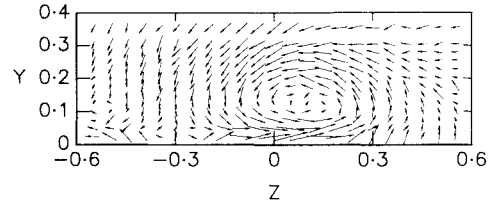

b) $X = 4.5$

Fig. 5 Secondary velocity vectors $(V^2 + W^2)^{1/2}/U_o$: the measurement point is at the center of the arrow; a length of 0.1 corresponds to a distance of 0.15 along the axis.

about $Y = 1.0$. This justification was reinforced by the small variation in C_l near the tunnel midplane, Figs. 2 and 3. Second, there was good symmetry about $Z = 0$ in the boundary-layer measurements at $X = 1.5$ when the wing was at zero incidence and, hence, had near-zero lift. Thus, any measured *asymmetry* with the wing at nonzero incidence cannot be attributed to geometric asymmetry or poor flow quality.

All mean velocity measurements reported here were obtained from a five-hole pressure probe whose tip had an outside diameter of 2.3 mm. The calibration and use of this probe, including corrections for mean shear effects, is described by Westphal et al.[16] The probe was held by a vertical, 6.35-mm-diam stem that was attached to an automated traverse located above the working section. This stem caused some interference at the upstream and first downstream stations, which will be noted later. Apart from this unquantifiable interference, the uncertainty in the mean velocity measurements is 0.5% of U_o. The downstream measurements were taken over rectangular planes bounded by $-Z_w \le Z \le Z_w$ and $0 \le Y \le Y_w$; Z_w was 2.2 and Y_w was 0.95, except for the measurements upstream of the wing, for which Z_w and Y_w were 2.0 and 0.975, respectively.

Turbulence measurements were made using a crossed hot-wire probe in the Y-Z plane on both sides of the airfoil at the position of maximum thickness and at $X = 0.58$, 1.50, and 2.96 in the downstream flow. For economy, only the results at $X = 2.96$ will be discussed here. The X-wire probe and the associated data acquisition and reduction techniques are described by Westphal et al.[17] and by Westphal and Mehta.[18] The probe, which was held by the stem described previously, was used in two orientations to obtain all of the mean velocities, five of the six Reynolds stresses and the corresponding triple products. Again, for reasons of economy, we do not discuss the triple products in this paper. All of the mean velocity and turbulence measurements can be obtained on floppy disk from either author. The uncertainty in the Reynolds stresses is 10% of the undisturbed C_f.

III. Results and Discussion

Typical surface pressure distributions for $\alpha = 10$ deg are shown in Fig. 2; note that $Y = 0$ indicates the position where the bottom of the tappings touched the floor and, in the interest of clarity, the results for most values of Y are omitted. The small chord prevented the installation of pressure tappings near the trailing edge, where, fortunately, C_p does not change significantly with Y. The lift coefficient C_l was deter-

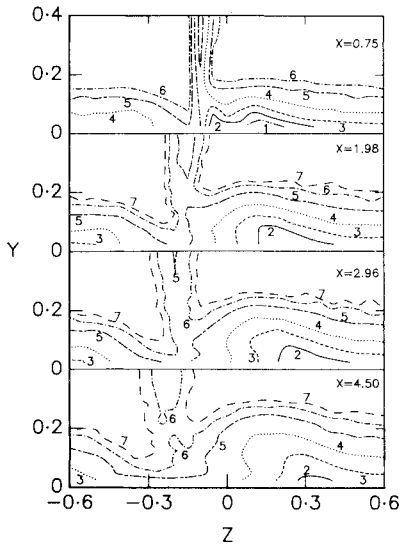

Fig. 6 Contours of mean streamwise velocity U/U_o downstream of the junction: 1, 0.50; 2, 0.60; 3, 0.70; 4, 0.80; 5, 0.90; 6, 0.95; 7, 0.975.

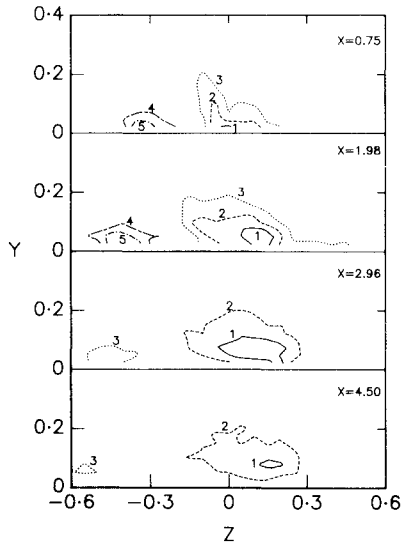

Fig. 7 Contours of mean streamwise vorticity $\Omega_x c/U_o$ downstream of the junction: contour levels for X = 0.75; 1, −0.30; 2, −0.20; 3, −0.10; 4, 0.10; 5, 0.20; contour levels for X = 1.98; 1, −0.15; 2, −0.10; 3, −0.05; 4, 0.05; 5, 0.10; contour levels for X = 2.96 and 4.5; 1, −0.10; 2, −0.05; 3, 0.05.

mined by trapezoidal integration of $C_P(x)$. The freestream C_{le}, determined at $Y = 0.95$, was 0.83. For $\alpha = 0$ and 5 deg, C_{le} was 0.03 and 0.51, respectively. The slightly low value at 10 deg (we expected a value close to 1) may be a consequence of the lack of resolution close to the leading edge where the suction and pressure peaks apparently have been poorly resolved. There is no evidence of any substantial laminar separation bubble on the wing. From the pressure distributions of Fig. 2, it is apparent that the lift coefficient is only slightly reduced at the surface; indeed, we found that C_l at $Y = 0$ is still 84% of C_{le}, a result that is consistent with the findings of Mendelsohn and Polhamus[22] and Sepri.[23] The ratio $[C_l(Y) - C_l(Y = 0)]/[C_{le} - C_l(Y = 0)]$ is plotted in Fig. 3. This quantity does not indicate the small overall decrease in C_l, but does show a persistence in the reduction in $C_l(Y)$ out to values of Y beyond the edge of the undisturbed boundary layer (about $Y = 0.2$). The smoothness of the results suggests that this reduction in $C_l(Y)$ outside the boundary layer is genuine and is, therefore, an indication of inviscid effects. The overall implication is that little of the bound vorticity is converted into trailing secondary vorticity and that most effectively passes through the surface to satisfy the inviscid condition that vortex lines cannot end in the fluid.

Figure 3 also gives the partial circulation $\gamma_m(Y)$ determined using a trapezoidal approximation to

$$\int_{-z_w}^{z_w} W(Y,Z)\, dZ$$

Typical spanwise profiles of W are shown in Figs. 4 for the minimum and maximum values of Y at each X. There is evidence of probe interference around $Z = -0.01$ just upstream and downstream of the wing (Figs. 4a and 4b), but the net effect on γ_m appears small. The straight, dashed lines in Fig. 3 denote the freestream partial circulation γ_e that would result from replacing the airfoil by a vortex at the quarter-chord position and considering the line along which γ_m is defined (a straight segment at fixed X and Y, bounded at $+/- Z_w$) to be part of a contour enclosing the airfoil in the X-Z plane. By ignoring the small displacement of the quarter-chord position from the tunnel centerline, it can be shown that

$$\frac{\gamma_e}{U_o c} = \frac{C_{le}}{2\pi} \arctan \frac{Z_w}{H} \tag{1}$$

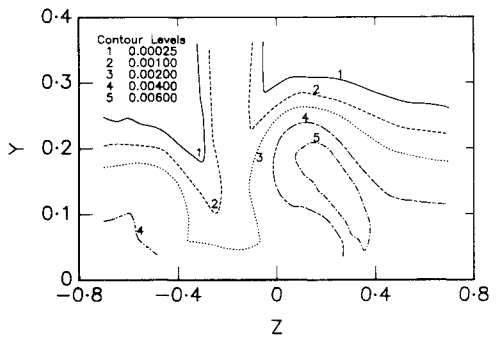

a) $\overline{u^2}/U_o^2$

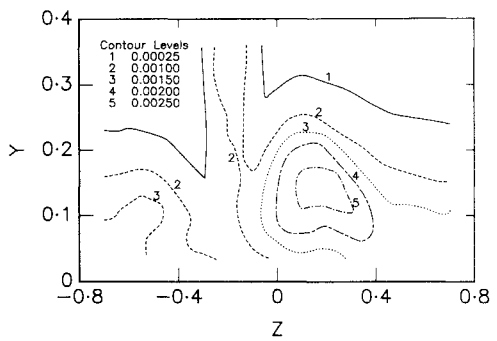

b) $\overline{v^2}/U_o^2$

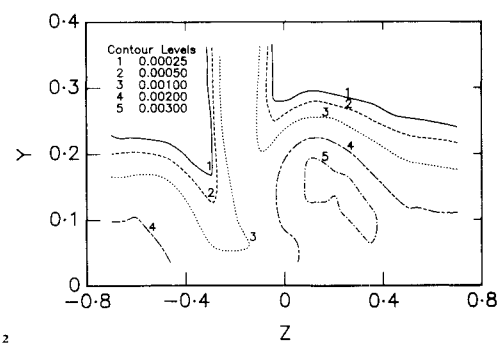

c) $\overline{w^2}/U_o^2$

Fig. 8 Contours of Reynolds normal stresses at X = 2.96.

where $H = (X + 0.25)$ is the streamwise distance from the vortex. [Note that by Eq. (1) γ_e is independent of Y and tends to half the bound circulation as $Z_w \to \infty$.] The corresponding equation for W,

$$\frac{W}{U_o} = \frac{C_{le}}{2\pi} \frac{H}{Z^2 + H^2} \tag{2}$$

is plotted in Figs. 4. Generally, the agreement between $\gamma_m(Y)$ and γ_e is remarkably good for $Y \geq 0.3$, where W/U_o is, typically, only 0.05. This small level means that γ_m cannot be expected to reflect the slight decrease in $C_l(Y)$ as Y decreases. Figures 4 also show the distribution of W determined from the two-dimensional panel code described by Moran.[24] Forty panels were used to simulate the airfoil surface, and the predicted results were scaled by the ratio of the predicted to measured C_{le}. There is little difference between the panel code predictions and Eq. (2), even though two of the three values of X used in Figs. 4 lie within 1 chord length of the wing.

Outside the boundary layer, γ_m is determined to first order by the nearly constant bound vorticity of the wing. The implication is that the strictly two-dimensional relationship between lift and circulation embodied in Eq. (1) remains a reasonable approximation. However, γ_m is also related to the axial vorticity in the boundary layer because it is the dominant contribution to the circulation around a rectangular contour in the Y-Z plane whose corners are $(Y, -Z_w)$, (Y, Z_w), $(0, Z_w)$, and $(0, -Z_w)$. Provided Z_w is sufficiently large and $Y > \delta_{99}/c$, this circulation equals the area integral of Ω_X within the boundary layer. We now consider the generation of this axial vorticity.

The maintenance of the wing's surface pressure distribution almost to the junction implies that the dominant pressure gradients remain in the X-Z plane even in the boundary layer and their magnitudes are preserved as the body is approached. We discuss first the response of the outer part of the boundary layer to those pressure gradients. The small radii of curvature for the streamlines close to the leading edge must cause the rapid conversion of cross-stream mean vorticity into the necklace or horseshoe vortex. (The details of the winding up depend on the leading-edge shape, as documented by Mehta.[6]) Farther from the wing, the secondary vorticity is too small to generate additional discrete vortices. As the outer streamlines pass downstream of the airfoil, their radii of curvature change sign. To the inviscid, small deflection approximation, the downstream crossflow will depend only on the net deflection and the upstream $\partial U/\partial Y$. Presumably, this is the reason for the crossflow profiles, particularly noticeable for $Z < -0.2$ in Fig. 5a, that are typical of the response of a two-dimensional boundary layer to lateral skewing, e.g., Bradshaw.[1,2] This crossflow occurs where the U contours are hardly disturbed, Fig. 6. A comparison of Figs. 5a and 5b shows that, as X increases, the magnitude of the crossflow decreases, as required by the previous argument.

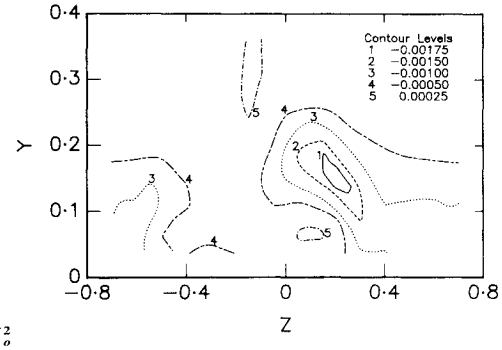

a) $\overline{uv}/U_o^2$

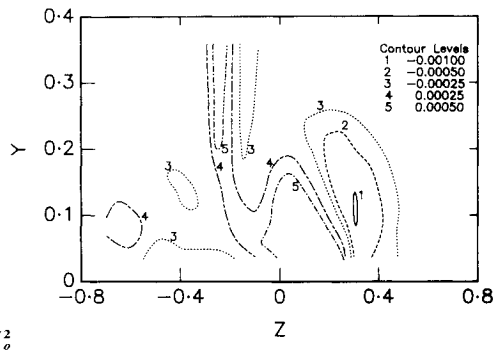

b) $\overline{uw}/U_o^2$

Fig. 9 Contours of Reynolds shear stresses at $X = 2.96$.

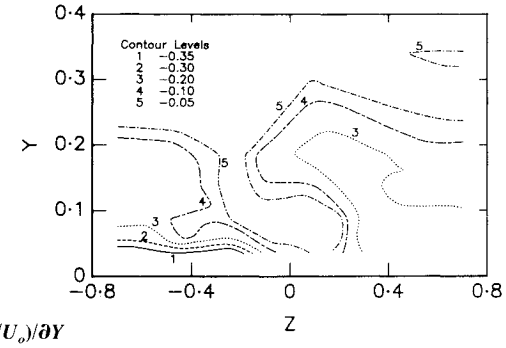

a) $\partial(U/U_o)/\partial Y$

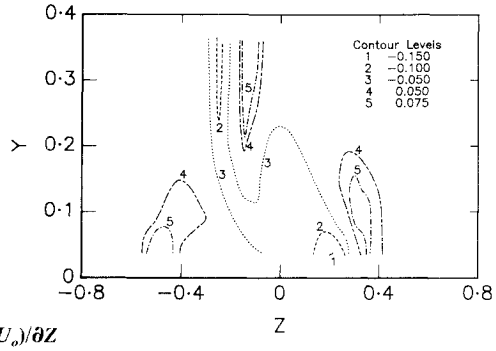

b) $\partial(U/U_o)/\partial Z$

Fig. 10 Contours of mean streamwise velocity gradients at $X = 2.96$.

At the body surface, the cross-stream momentum equation reduces to

$$\nu \frac{\partial \Omega_X}{\partial Y} = \frac{1}{\rho} \frac{\partial P}{\partial Z} \tag{3}$$

Thus, somewhat paradoxically, streamwise vorticity must be generated at the surface to maintain the wing surface pressure. It is interesting that the equivalent form of Eq. (3) is recovered if the Navier-Stokes equations are written in orthogonal, curvilinear coordinates, two of which lie in the plane of the floor (body) and the third in the Y direction. In other words, Ω_X cannot be generated in the near-wall region by the streamline curvature terms similar to those responsible for the skewing in the outer layer, even though both sources of Ω_X arise from the cross-stream pressure gradient. (We discount as unlikely any significant generation of Ω_X arising from the turbulence stresses.) Bradshaw[1] pointed out that the sign of Ω_X generated near the wall is usually opposite to that of Ω_X in the outer layer. We could not probe the wall region; this argument is provided to show that the downstream behavior of γ_m is likely to reflect some interaction, perhaps cancellation, of Ω_X from the two sources.

From this, it appears reasonable to suppose that γ_m has two main components. The first, attributable to the bound vorticity of the wing, is approximately constant with Y, and so

must also be related to the axial vorticity generation at the body surface. The second is caused by the skewing of the outer boundary layer near the wing's leading edge as well as the generation of Ω_X near the wall, and tends to zero outside the boundary layer. This division would explain the observation that W and γ_e do not vary significantly with Y upstream of the wing, as the minimum Y for those measurements was in the outer portion of the boundary layer. It is consistent with the analysis of the flow around surface mounted obstacles by Mason and Morton.[25] They showed that the skew-induced vorticity does not contribute to the global circulation in the Y-Z plane, that is, to γ_m (Y) in the limit as Y and $Z_w \to \infty$. Their other result, that the global circulation is zero, obviously does not apply to our case where there is circulation at $X = -\infty$ due to the bound vorticity of the wing.

Figure 6 also shows the limited region of interaction between the disturbed boundary layer and the wake: the latter being easily delineated by the nearly vertical contours at large Y. Note that the center of the wake is progressively deflected in the negative Z direction as a consequence of the lift of the wing. A comparison with Fig. 7 shows that the region where the boundary layer has been thinned, around $Z = -0.2$, separates the regions of positive and negative vorticity. These regions also appeared in X-wire measurements (which are not shown here) at the position of maximum airfoil thickness, $X \sim -0.2$, the closest measurement plane to the leading edge. They can, therefore, be associated with the two legs of the skew-induced vortex formed near the leading edge. The larger magnitude of the suction surface leg agrees with the model proposed by Young.[8] Figure 7 shows a decrease in the vorticity levels in both legs as X increases, and a movement apart as would be expected for the case of a vortex pair with the common flow toward the wall, e.g., Pauley and Eaton.[19]

The three normal stresses measured at $X = 2.96$ are shown as contour plots in Figs. 8, and the two measured turbulence shear stresses are shown in Figs. 9. As expected from Fig. 7, the suction leg dominates the turbulence distribution. This leg has ingested the wake, but in such a way as to preserve the qualitative features of a flow with a single imbedded vortex, e.g., Shabaka et al.[14] and Westphal et al.[16] As for the single vortex, the distributions of $\partial U/\partial Y$ (Fig. 10a) and $\partial U/\partial Z$ (Fig. 10b) are qualitatively similar to those of $\overline{uv}$ and $\overline{uw}$, respectively, indicating that an eddy viscosity model may be appropriate in the downstream flow.

There is a region between the vortices where $\overline{uv}$ is very small, Fig. 9a. Both the mean flow and turbulence measurements show that the boundary layer between the vortices has been thinned and is diverging as the two vortices move apart. This region also contains part of the ingested wake, as shown by the contours of $\overline{uw}$, Fig. 9b, which is the primary shear stress in the wake well away from the floor. However, the contours of $\overline{uv}$ and $\overline{uw}$ for positive Z are typical of single vortex flows. The region of negative $\overline{uw}$ around $Z = 0.3$ (see Fig. 9b) occurs where both $\partial U/\partial Z$, Fig. 10b, and $\overline{w^2}$, Fig. 8c, are large, in good agreement with the trends for the single vortex.[14,16]

IV. Conclusions

The remarkably small decrease in the wing's surface pressure and section lift coefficient near the junction implies that little bound vorticity is trailed into the downstream flow. As a consequence, the partial cross-stream circulation, measured at constant height outside the boundary layer, was determined largely by the bound circulation of the airfoil, which is consistent with the constraint proposed by Mason and Morton.[25] The partial circulation is also related to the axial vorticity in the body boundary layer. This vorticity was formed by a combination of direct generation by the cross-stream pressure gradients near the body surface and the skewing of the circumferential vorticity in the outer layer. The former mechanism was apparently dominant at the single upstream measuring station, 1 chord length from the leading edge, but it was not possible to distinguish the relative importance in the downstream flow.

Downstream of the wing, the disturbed body boundary layer is dominated by the two legs of the necklace vortex formed near the leading edge. The suction surface leg is the stronger, as was originally suggested by Young,[8] but the vorticity levels decrease in both legs with increasing distance from the wing. The interaction of the wing wake and the boundary layer is confined to a narrow region between the legs. The wake is distorted in the direction of the suction leg, but does not appear to have a strong influence on it.

The turbulence measurements at stations beyond 2 chord lengths downstream of the trailing edge confirm the small effects of the wing wake on the longitudinal vortex flow. In this region, the suction leg has the general features of an isolated vortex in a turbulent boundary layer and the boundary layer between the two vortices is thinning as the flow diverges. At least qualitatively, the measured shear stresses are distributed in accordance with an eddy viscosity turbulence model.

Acknowledgments

D. H. Wood was supported by a National Research Council-NASA Research Associateship during the course of this work. The panel code calculations were done by G. Gordon.

References

[1]Bradshaw, P., "Turbulent Secondary Flows," *Annual Review of Fluid Mechanics*, Vol. 19, 1987, pp. 53–74.

[2]Bradshaw, P., "Physics and Modelling of Three-Dimensional Boundary Layers," VKI Lecture Series, 1986.

[3]Shabaka, I. M. M. A., and Bradshaw, P., "Turbulent Flow Measurements in an Idealized Wing/Body Junction," *AIAA Journal*, Vol. 19, No. 2, 1981, pp. 131, 132.

[4]Nakayama, A., and Rahai, H. R., "Measurement of Turbulent Flow Behind a Flat Plate Mounted Normal to the Wall," *AIAA Journal*, Vol. 22, No. 12, 1984, pp. 1817–1819.

[5]Kubendran, L. R., McMahon, H. M., and Hubbartt, J. E., "Turbulent Flow Around a Wing-Fuselage Type Juncture," AIAA Paper 85-0040, 1985.

[6]Mehta, R. D., "Effect of Wing Nose Shape on the Flow in a Wing/Body Junction," *Aeronautical Journal of the Royal Aeronautical Society*, Vol. 88, 1984, pp. 456–460.

[7]Hawthorne, W. R., "The Secondary Flow About Struts and Airfoils," *Journal of Aerospace Sciences*, Vol. 21, 1954, pp. 588–608.

[8]Young, A. D., "Some Special Boundary Layer Problems," *Zeitschrift für Flugwissenschaften und Neltraumforschung.*, Vol. 6, Nov. – Dec. 1977, pp. 401–414.

[9]Barber, T. J., "An Investigation of Strut-Wall Intersection Losses," *Journal of Aircraft*, Vol. 15, No. 10, 1978, pp. 676–681.

[10]Özcan, O., and Ölcmen, M. S., "Measurements of Turbulent Flow Behind a Wing-Body Junction," *AIAA Journal*, Vol. 26, No. 4, 1988, pp. 494–496.

[11]Kuchemann, D., *The Aerodynamic Design of Aircraft*, Pergamon, Oxford, England, UK, 1978.

[12]Ashley, H., and Rodden, W. P., "Wing-Body Aerodynamic Interaction," *Annual Review of Fluid Mechanics*, Vol. 4, 1972, pp. 431–472.

[13]Moore, J., and Ransmayr, A., "Flow in a Turbine Cascade: Part 1—Losses and Leading Edge Effects," *Journal of Engineering for Gas Turbines and Power*, Vol. 106, No. 3, 1984, pp. 400–408.

[14]Shabaka, I. M. M. A., Mehta, R. D., and Bradshaw, P., "Longitudinal Vortices Imbedded in Turbulent Boundary Layers. Part 1: Single Vortex," *Journal of Fluid Mechanics*, Vol. 155, June 1985, pp. 37–57.

[15]Mehta, R. D., and Bradshaw, P., "Longitudinal Vortices Imbedded in Turbulent Boundary Layers. Part 2: Vortex Pair with 'Common Flow' Upwards," *Journal of Fluid Mechanics*, Vol. 188, March 1988, pp. 529–546.

[16]Westphal, R. V., Pauley, W. R., and Eaton, J. K., "Interaction Between a Vortex and a Turbulent Boundary Layer. Part 1: Mean Flow Evolution and Turbulence Properties," NASA TM-88361, Jan. 1987.

[17]Westphal, R. V., Eaton, J. K., and Pauley, W. R., "Interaction Between a Vortex and a Turbulent Boundary Layer in a Streamwise Pressure Gradient," *Turbulent Shear Flows*, Vol. 5, edited by F. Durst, Springer-Verlag, New York, 1987, pp. 266–277.

[18]Westphal, R. V., and Mehta, R. D., "Interaction of an Oscillating Vortex with a Turbulent Boundary Layer," *Experiments in Fluids*, Vol. 7, No. 6, 1989, pp. 405–411.

[19]Pauley, W. R., and Eaton, J. K., "Experimental Study of the Development of Longitudinal Vortex Pairs in a Turbulent Boundary Layer," *AIAA Journal*, Vol. 26, No. 7, 1988, pp. 816–823.

[20] Westphal, R. V., "Skin Friction and Reynolds Stress Measurements for a Turbulent Boundary Layer Following Manipulation Using Flat Plates," AIAA Paper 86-0283, Jan. 1986.

[21]Wood, D. H., and Westphal, R. V., "Measurements of the Free Stream Fluctuations Above a Turbulent Boundary Layer," *Physics of Fluids*, Vol. 31, No. 10, 1988, pp. 2834–2840.

[22]Mendelsohn, R. A., and Polhamus, J. F., "Effects of the Tunnel-Wall Boundary Layer on Test Results of a Wing Protruding from a Wall," NACA TN 1244, Jan. 1947.

[23]Sepri, P., "An Investigation of the Flow in the Region of the Junction of a Wing and a Flat Plate Normal to the Wing Span," Dept. of Aeronautical Engineering, Queen Mary College, London, Rept. QMC ER-1002, Aug. 1973.

[24]Moran, J., *An Introduction to Theoretical and Computational Aerodynamics*, Wiley, New York, 1984.

[25]Mason, P. J., and Morton, B. R., "Trailing Vortices in the Wakes of Surface-Mounted Obstacles," *Journal of Fluid Mechanics*, Vol. 175, Feb. 1987, pp. 247–293.